BIOLOGIJA
2024. Vol. 70. No. 4. P. 163–179

ISSN 1392-0146 eISSN 2029-0578
DOI: https://doi.org/10.6001/biologija.2024.70.4.1

Screening the phytochemical components of *Ruta montana* L. for their inhibitory activity to reduce the progress of osteoarthritis: an *in silico* study

Imane Abdelli[1, 2*],

Faiçal Hassani[2],

Sarra Ghalem[2],

Sohayb Bekkal Brikci[2],

Ihab Sid Ahmed Nour[2],

Andrés Reyes Chaparro[3],

Amina Belhadji[2],

Mohamed El Hadi Ghalem[4],

Abdelkarim Ferouani[2]

[1] *Higher School of Applied Sciences, Tlemcen, Algeria*

[2] *University of Tlemcen, Tlemcen, Algeria*

[3] *National Autonomous University of Mexico, Mexico, Mexico*

[4] *Hospital of Tlemcen, Tlemcen, Algeria*

The species *Ruta montana* L. is well known for its medicinal characteristics. It is employed in traditional medicine where its constituent parts include a variety of physiologically active chemicals that give it its therapeutic potential. Our *in silico* research on the ligand molecules of *R. montana* L. shows the inhibitory efficacy of these compounds on the enzymes aggrecanase-1 (ADAMTS-4) and aggrecanase-2 (ADAMTS-5) responsible for the degradation of human articular cartilage in osteoarthritis. By using molecular docking simulation, the interaction between the ligand molecules of the plant researched and these enzymes was identified. These compounds scored higher in the *in silico* research of the components 2-Undecanol acetate, 2-Nonanol acetate, Nonan-2-one, Psoralen, and Undecan-2-one, corresponding to a larger inhibitory activity when compared to those of the commercially available medications for osteoarthritis.

Keywords: *Ruta montana* L. components, osteoarthritis, aggrecanase-1 (ADAMTS-4), aggrecanase-2 (ADAMTS-5), molecular docking simulation

* Corresponding author. Email: i_abdelli@yahoo.fr

INTRODUCTION

The most prevalent rheumatic condition, osteoarthritis, affects many elderly people. The interphalangeal, carpometacarpal, spine, hip, and first metatarsophalangeal joints are frequently affected, although the ankle, wrist, and elbow joints are typically spared (barring direct damage). Osteoarthritis is brought on by mechanical and biological events that upset the delicate balance between cartilage and subchondral bone formation and breakdown (Neogi, 2013).

Articular cartilage degeneration leads to osteoarthritis. The chondrocyte that makes up articular cartilage is encased in an extracellular matrix (ECM). Collagen and proteoglycans, such as aggrecan, make up the ECM (Vincent et al., 2022).

Pre-arthritic aggregate breakdown of articular cartilage occurs with osteoarthritis (Malfait et al., 2008). This is caused by the activity of aggrecanases, a class of proteolytic enzymes, especially aggrecanase-1 (ADAMTS-4) and aggrecanase-2 (ADAMTS-5). They have been recognised as the principal enzymes in cartilage breakdown (Chen et al., 2014). Finding drugs that can slow the progression of diseases or drugs that can treat diseases is a critical problem today. Targets include reducing cartilage degradation and encouraging regeneration.

Our research focuses on the inhibition of aggrecanase-1 and aggrecanase-2 by ligands derived from essential oils of *Ruta montana* (Table 1) and aims to identify new potential therapeutics for the treatment of arthrosis (Ihab, 2020).

Table 1. **Essential oils of *R. montana* (Kambouche et al., 2008)**

	Ligands	Kovats index	Percentage %
1	2-Nonanol acetate	1.230	18.20
3	2-Undecanol acetate	1.426	4.02
14	Nonan-2-one	1.089	29.54
17	Psoralen	2.099	3.52
19	Undecan-2-one	1.291	32.81

In light of the significant therapeutic potential of this plant, we suggested conducting a comparison study between molecules isolated from *R. montana* and drugs with anti-inflammatory properties (Mohhr et al., 1982; Juan et al., 1984) that are used to treat osteoarthritis pain. The goal of this comparison is to find new molecules of *R. montana* that can limit the activity of the two enzymes aggrecanase-1 (ADAMTS-4) and aggrecanase-2 (ADAMTS-5), which are thought to be the primary causes of arthritic disease and are responsible for cartilage degradation.

MATERIALS AND METHODS

For this investigation, the *in silico* study methodologies comprised several steps.

Enzyme preparation

The study used the enzymes aggrecanase-1 (ADAMTS-4) and aggrecanase-2 (ADAMTS-5) (Fig. 1). 3D structures of these enzymes are available for download as extension files from

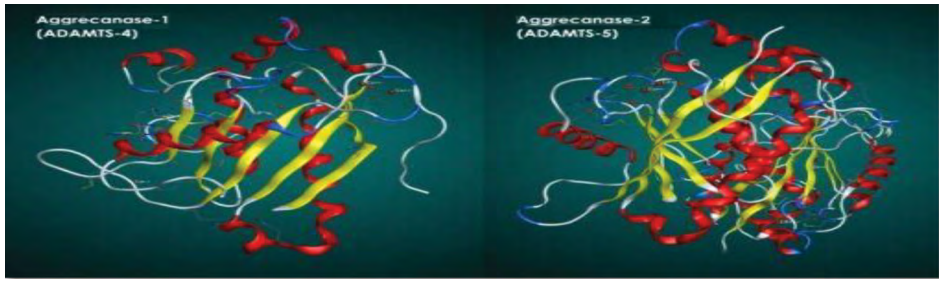

Fig. 1. 3D structures of aggrecanase-1 (ADAMTS-4) and aggrecanase-2 (ADAMTS-5) (Protein Data Bank)

the database (PDB) (.pdb). According to studies by Raghavet et al., 2006 and Kuzovkina, et al., 2009, the ideal resolution for investigations is typically between 1.5 Å and 2.5 Å. Based on this principle, we selected the structures having the characteristics listed in Table 2.

Preparation of ligands and drugs

The structures of the ligand molecules of *R. montana* (Fig. 2), the drugs compared (Fig. 3), and the co-crystallisation ligands (Fig. 4) are available for download from the database (PubChem) under forms extension files (sdf).

After downloading the molecule structures, we used ChemDraw Ultra to convert the structure files into files with the extension (.chm), and then we used Hyperchem 8.0.8 software (Mejri et al., 2010) to optimise the geometrical shapes of the structures and save them as files (.mol). The resulting files (.mol) were taken to the Molecular Operating Environment (MOE) for structural correction and protonation, followed by energy reduction, where they were saved as optimised structures in molecular database files (.mdb) and made available for molecular docking simulation.

Table 2. **Properties of aggrecanase-1(ADAMTS-4) and aggrecanase-2 (ADAMTS-5)**

Enzyme	ID PDB	Classification	Method	Resolution	Number of chains	Chain length
ADAMTS-4	4WKE	Hydrolase	X-ray diffraction	1.62Å	1	235
ADAMTS-5	3HY7	Hydrolase	X-ray diffraction	1.69Å	2	442

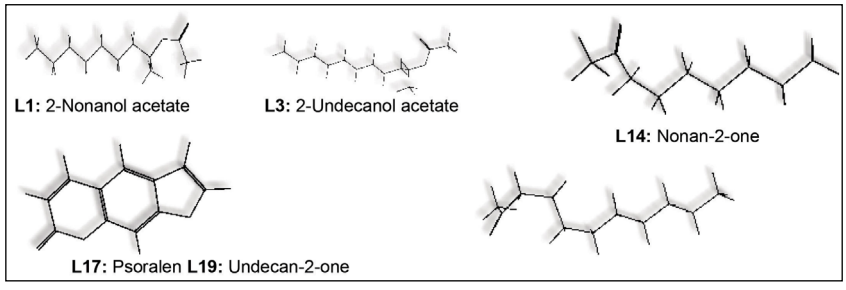

Fig. 2. *R. montana*. Structures of essential oils

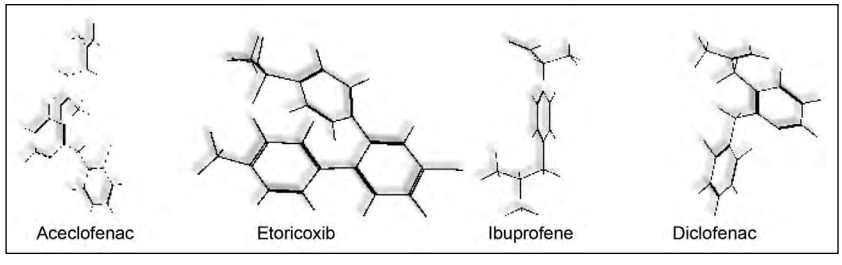

Fig. 3. Chemical structures of *R. montana* drug

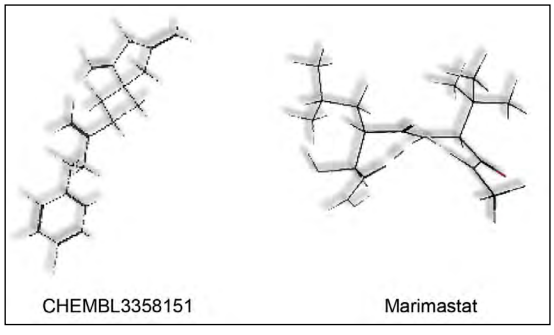

Fig. 4. Co-crystallisation ligand structures of aggrecanase-1 (ADAMTS-4) and aggrecanase-2 (ADAMTS-5)

Molecular docking simulation

Docking is a method that predicts (Clément, Slenzka, 2006) the most favourable orientation of a molecule with respect to another in order to have the most stable complex (Didierjean, Tête-Favier, 2016). It allows to predict the affinity of these molecules (HyperChem v8. Molecular Modelling System, Hypercube Inc, 2009) and Trouillas (2011).

After preparing the enzymes, plant ligands, drugs, and co-crystallisation ligands, we performed the molecular docking using MOE software package (Attaf., 2010), this process can be summarised in two steps:

➢ Docking is the selection stage, which consists of placing the ligand in the active site of the protein and sampling the possible conformations, positions, and orientations (poses), retaining only those that represent the most favourable modes of interactions.

➢ Scoring is the ranking stage, which consists in evaluating the affinity between the ligand and the protein and giving a score to the poses obtained during the docking phase. This score will enable the best pose among all those proposed to be selected (Fig. 5).

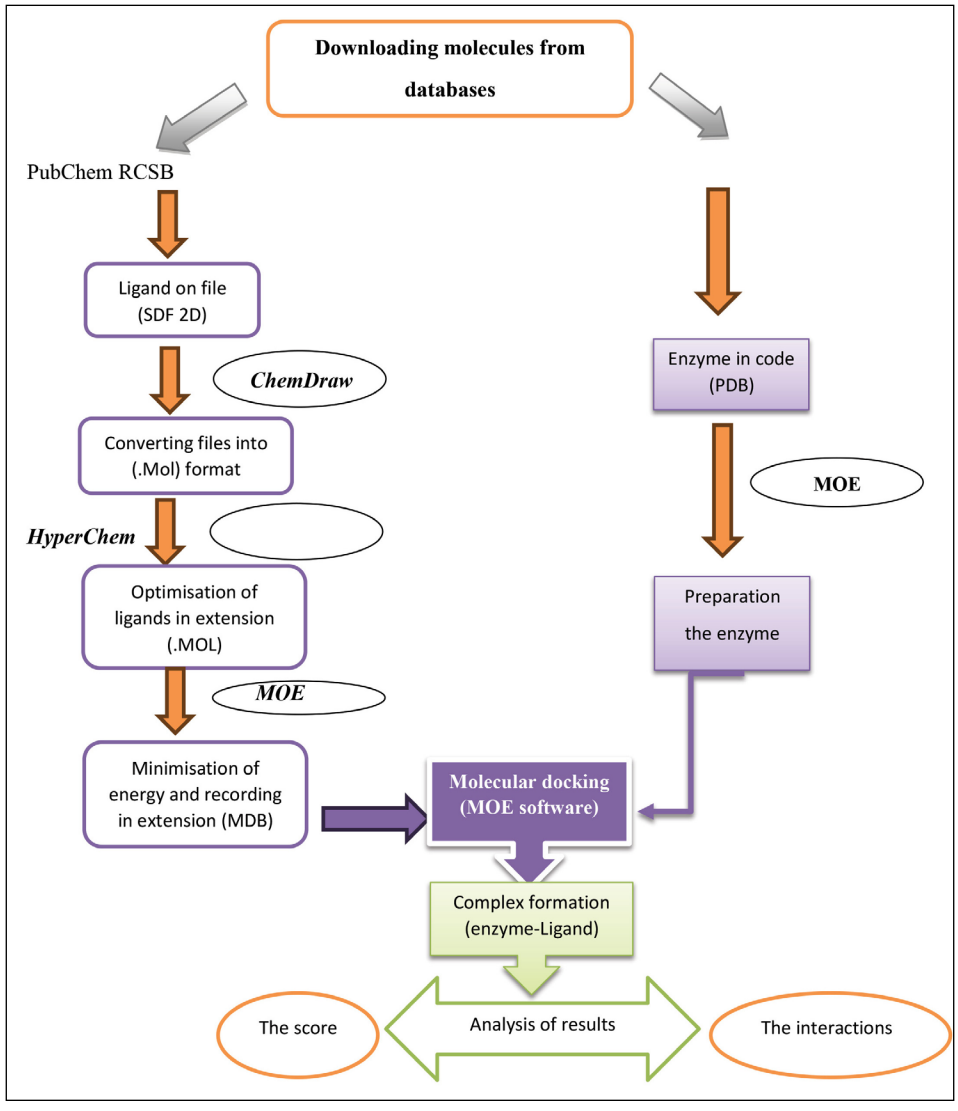

Fig 5. Molecular docking protocol

Molecular dynamics simulations

Molecular dynamics tests were done to determine the stability of the ligand-receptor complexes resulting from molecular docking tests. The CHARMM-GUI platform was used to prepare the different inputs, and software GROMACS (2021) (Jo et al., 2008; Abraham et al., 2015; GROMACS, 2021). Using the PDB reader tool, each protein underwent preprocessing (Jo et al., 2014). On the other hand, using (OpenBabel), the docking ligands that had the highest affinity energy were chosen (O'Boyle et al., 2011).

The ligand mol2 files were loaded into the (Ligand Reader & Modeler) tool to generate the parameters and topology files (Kim et al., 2017). The ligand-receptor complexes were integrated into a single .pdb file for use in the Solution Builder tool to create the system that was used as input for GROMACS (Lee et al., 2016). Water box was cubic, fit to protein size, and 10 Å of edge distance. Each system was neutralised using KCl ions placed by Monte-Carlo method, at concentration of 0.15 M. Each system underwent 5000 steps of steepest descents energy minimisation to remove steric overlap. Afterwards, all the systems were subjected to an NVT (constant number of particles, volume, and temperature) equilibration phase for 125000 steps, using the V-rescale temperature-coupling method, with constant coupling of 1 ps at 303.15 K (Bussi et al., 2007). Subsequently, the molecular dynamics was carried out for 100 ns using the CHARMM36m force field (Vanommeslaeghe et al., 2010).

GROMACS utilities were used to evaluate the root-mean-square deviation (RMSD) of the complexes, as well as that of each protein and ligand, root-mean-square fluctuation (RMSF), and hydrogen bonds. The data were graphed using the GRACE program. The evaluation of free energy of binding (ΔGBind) of the ligand-receptor complexes was carried out using 'Molecular Mechanics Poisson-Boltzmann Surface Area' (MM-PBSA) using the open-source g_mmpbsa package (Baker et al., 2001; Kumari et al., 2014).

The MM-PBSA calculations

This energy of protein-ligand complexes can be calculated by combining molecular mechanics/Poisson-Boltzmann surface analysis (MM-PBSA) with MD. MD scripts were extracted to perform MM-PBSA calculations. The offered insights into existing biomolecular interactions. The MM-PBSA binding free energies were calculated using the script 'g_mmpbsa' (Kumari, Kumar, Lynn, 2014) in GROMACS. The calculations of energy in this method were done by the following equation:

$$\Delta G_{binding} = G_{complex} - (G_{receptor} + G_{ligand})$$

where the $\Delta G_{binding}$ represents the total binding energy of the complex, $G_{receptor}$ the binding energy of free receptor (Tanuja, 2021), and G_{ligand} that of unbounded ligand.

RESULTS AND DISCUSSION

Molecular docking simulation

After docking for all molecules, we obtained the results presented below in the Table 3. According to the results, the ligand with the lowest score, which corresponds to the most stable conformation within the receptor with the lowest energy will be chosen to form the most stable ligand-enzyme complex.

The parts of the plant are graded in ascending order, with the best enzyme inhibitor having the lowest score. The following compounds are listed in ascending order by index for docking with the enzyme aggrecanase-1 (ADAMTS-4): L3, ligand of co-crystallisation, Aceclofenac, L19, L1, Ibuprofen, and L17, L14, Diclofenac (Ihab, 2020). After observing the above (Table 3), we concluded that the best score corresponds to the plant component L3 (2-Undecanol acetate) estimated by –7.0724797 Kcal/mol, followed by the co-crystallisation ligand (CHEMBL3358151) with a value of –6.914968 Kcal/mol, while the best drug score is that of Aceclofenac in the third position with an estimation of –6.8224053 Kcal/mol. Two other ligands corresponding to

Table 3. **Docking score results of molecules with the enzyme aggrecanase-1 (ADAMTS-4), (Ihab, 2020)**

No.	Index	Ligands	Score				
			R. montana ligands	Co-crystallisation ligand	Drugs		
					Aceclofenac	Ibuprofen	Diclofenac
1	L3	2-Undecanol acetate	–7.0724797	–6.914668	–6.8224053	–6.2237363	–5.61990261
5	L19	Undecan-2-one	–6.3589239				
6	L1	2-Nonanol acetate	–6.2693677				
9	L17	Psoralen	–5.8345952				
11	L14	Nonan-2-one	–5.6666312				

the plant came before the second-best drug Ibuprofen –6.2237363 Kcal/mol are L19 and L1 with the scores –6.3589239 Kcal/mol and –6.2693677 Kcal/mol.

To conclude, we establish the following results for aggrecanase-1 (ADAMTS-4) inhibitors where we have: one plant ligand first superior to the co-crystallisation ligand, and the first drug; five plant ligands superior to the second drug; five plant ligands superior to the third drug; eight plant ligands repeating the last rankings.

Table 4 below represents the docking score of molecules with the enzyme aggrecanase-2 (ADAMTS-5).

For docking with the enzyme aggrecanase-2 (ADAMTS-5), the ascending order by index is: L3 Ibuprofen < L1 < Aceclofenac < L19 < Ligand of co-crystallisation < L14 < L17 < Etoricoxib.

The results of Table 4 above show that the best score is that of the ligand of the plant L3 (2-Undecanol acetate) with an estimated value of –6.8743758 Kcal/mol.

Regarding the docking results of aggrecanase-2 (ADAMTS-5), we concluded the following:

one ligand of the plant in the first place in addition to two others is superior to the first drug;

a ligand of the plant is superior to the second drug;

five ligands of the plant are superior to the co-crystallisation ligand;

ten ligands of the plant superior to the third drug which took the last place.

Table 4. **Docking results with the enzyme aggrecanase-2 (ADAMTS-5) (Ihab, 2020)**

No.	Index	Ligands	Score				
			Ruta montana ligands	Co-crystallisation ligand	Drugs		
					Ibuprofen	Aceclofenac	Etoricoxib
1	L3	2-Undecanol acetate	–6.8743758	–5.809947	–6.7959991	–6.7402992	–4.55266476
2	L1	2-Nonanol acetate	–6.7658854				
3	L19	Undecan-2-one	–6.4715576				
4	L14	Nonan-2-one	–5.67018600				
5	L17	Psoralen	–5.6021357				

Our aim was to confirm that the *R. montana* lant represents a realistic and adequate source of enzyme inhibitors responsible for osteoarthritis and a reference that is worth exploring in the field of drug synthesis, which brings us to the reason why the ligands with the highest scores are the main objective of the study.

According to the conclusion established above, the complexes formed for the selected molecules are represented in the Fig. 6 and Fig. 7.

The following results presented in Table 5 and Table 6 represent a comparison of the different complexes presented earlier.

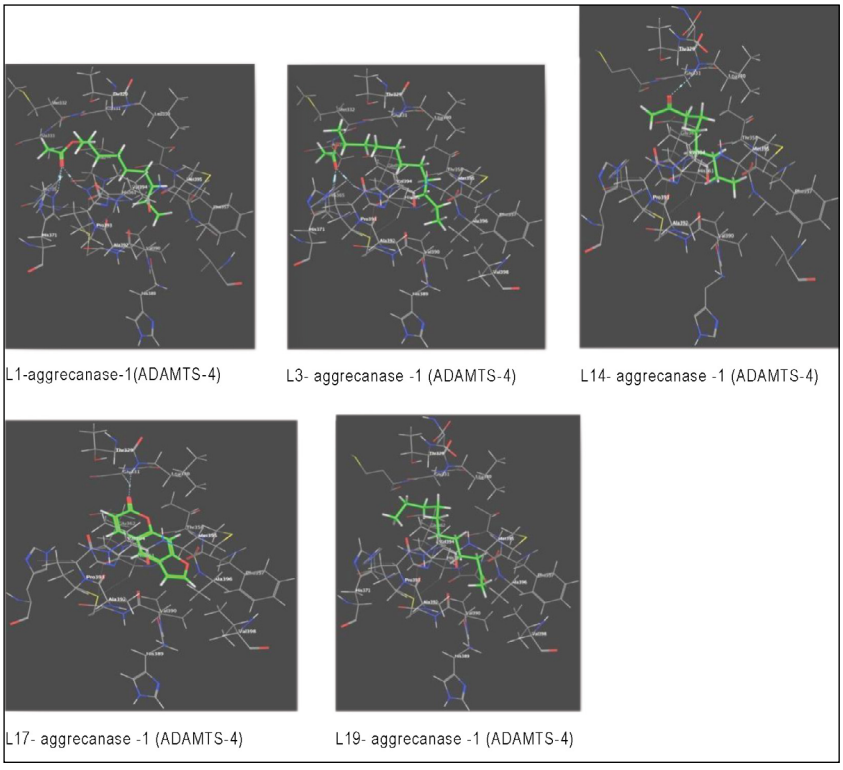

Fig. 6. Complexes formed with aggrecanase-1 (ADAMTS-4)

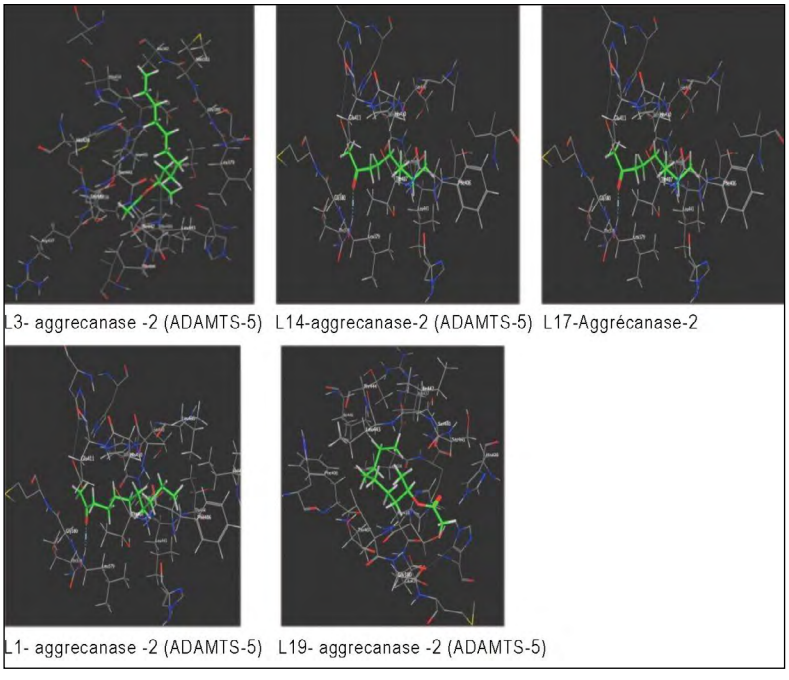

Fig. 7. Complexes formed with aggrecanase-2 (ADAMTS-5)

Table 5. **Comparison of the complexes formed with aggrecanase-1 (ADAMTS-4)**

	No.	Molecules	Score (Kcal/mol)	Interaction with residues site	Interaction types	Distance (Å)	Energies (kcal-mol)
Ligands	1	2-Undecanol acetate	–7.0724797	NE2-HIS361	H-acceptor	3.02	–3.0
				NE2-HIS365	H-acceptor	2.88	–3.7
				NE2-HIS371	H-acceptor	2.93	–3.8
	2	Undecan-2-one	–6.3589239	5-ring-HIS361	H-pi	3.77	–0.8
	3	2-Nonanol acetate	–6.2693677	NE2-HIS361	H-acceptor	3.09	–1.8
				NE2-HIS365	H-acceptor	3.31	–1.3
				NE2-HIS371	H-acceptor	2.96	–3.1
	4	Psoralen	–5.8345952	N-LEU330 CG-MET395	H-acceptor pi-H	3.19	–0.8
						3.84	–0.7
				5-ring-HIS361	pi-pi pi-pi	3.76	–0.0
				5-ring-HIS361		4.00	–0.0
	5	Nonan-2-one	–5.6666312	N-LEU330	H-acceptor	3.38	–0.9
				5-ring-HIS361	H-pi	3.70	–0.9
Drugs	6	Aceclofenac	–6.8224053	N-MET395	pi-H	4.64	–0.6
	7	Ibuprofen	–6.2237363	NE2-HIS361	H-acceptor	3.01	–7.3
				NE2-HIS365	H-acceptor	3.55	–1.1
				NE2-HIS371	H-acceptor	2.96	–3.7
	8	Diclofenac	–5.61990261	CA-VAL394	pi-H	4.01	–0.7
Ligand of co-cristalisation	9	CHEMBL3358151	–6.914968	/	/	/	/

Table 6. **Comparison of the complexes formed with aggrecanase-2 (ADAMTS-5)**

	No.	Molecules	Score (Kcal/mol)	Interaction with residues site	Interaction types	Distance (Å)	Energies (kcal-mol)
Ligands	1	2-Undecanol acetate	–6.8743758	5-ring-HIS410 (B)	H-pi	3.81	–1.1
	2	2-Nonanol acetate	–6.7658854	/	/	/	/
	3	Undecan-2-one	–6.4715576	N-LEU379 (B)	H-acceptor	3.00	–3.3
				5-ring-HIS410 (B)	H-pi	4.09	–1.0
	4	Nonan-2-one	–5.67018600	N-LEU379 (B)	H-acceptor	2.99	–3.4
				5-ring-HIS410 (B)	H-pi	3.78	–1.2
	5	Psoralen	–5.6021357	5-ring-HIS410 (B)	pi-pi	3.89	–0.0
Drugs	6	Ibuprofen	–6.7959991	NE2-HIS410 (B)	H-acceptor	2.91	–2.5
				NE2-HIS410 (B)	H-acceptor	3.11	–4.7
				NE2-HIS410 (B)	H-acceptor	2.92	–4.4
				5-ring-HIS410 (B)	pi-pi	3.63	–0.0
	7	Aceclofenac	–6.7402992	5-ring-HIS410 (B)	H-pi	3.58	–0.6
	8	Etoricoxib	–4.55266476	CG2-ILE442 (B)	H-acceptor	3.50	–2.1
				CA-ILE442 (B)	pi-H	4.75	–1.0
				CB-LEU443 (B)	pi-H	4.47	–0.6

Table 6. **(Continued)**

	No.	Molecules	Score (Kcal/mol)	Interaction with residues site	Interaction types	Distance (Å)	Energies (kcal-mol)
Ligand of co-cristalisation	9	Marimastat	–5.809947	OD2-ASP422 (B) OG-SER441 (B) NH1-ARG285 (A)	H-donor H-donor H-acceptor	2.84 3.22 3.08	–2.8 –1.6 –1.0

The interactions between 2.5 Å and 3.1 Å are considered strong and those between 3.1 Å and 3.55 Å are assumed to be medium. Interactions greater than 3.55 Å are weak or absent (Ihab, 2020).

For the enzyme aggrecanase-1 (ADAMTS-4), the ligands of the plant 2-Undecanol acetate and 2-Nonanol acetate show three same interactions of the H-acceptor type with the residues HIS361, HIS365, and HIS371 as the Ibuprofen drug. The Undecan-2-one ligand is formed by an H-pi interaction with the amino acid HIS361, while the Psoralen is formed by four interactions, one with LEU330, one with MET395, and two interactions with the residue HIS361. On the other hand, Nonan-2-one has two interactions with LEU330 and HIS361. The drugs Aceclofenac and Diclofenac each formed an interaction, the first with MET395 and the second with residue VAL394, while the reference ligand CHEMBL3358151 had no interactions. The distances between the ligands of the plant and the amino acids of the active site of the enzyme ADAMTS-4 vary between 2.88 Å and 4.00 Å, while the distances between the drugs fluctuate between 2.96 Å and 4.64 Å, which indicates that plant ligands have stronger interactions than those of drugs, where the best score ligand having a strong interaction with HIS365, due to a distance of 2.88 Å and an energy of –3.7 kcal/mol. The 2D representations of the best pose interactions between the ligands and their receptor ADAMTS-4 are presented in Figs 8–10.

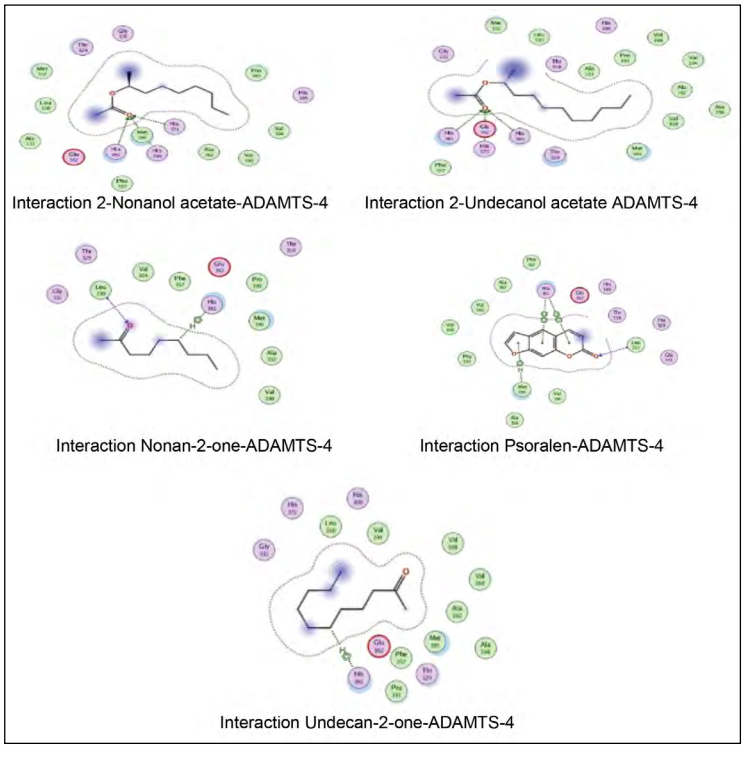

Fig. 8. 2D representations of the best pose interactions between *R. montana* ligands and ADAMTS-4

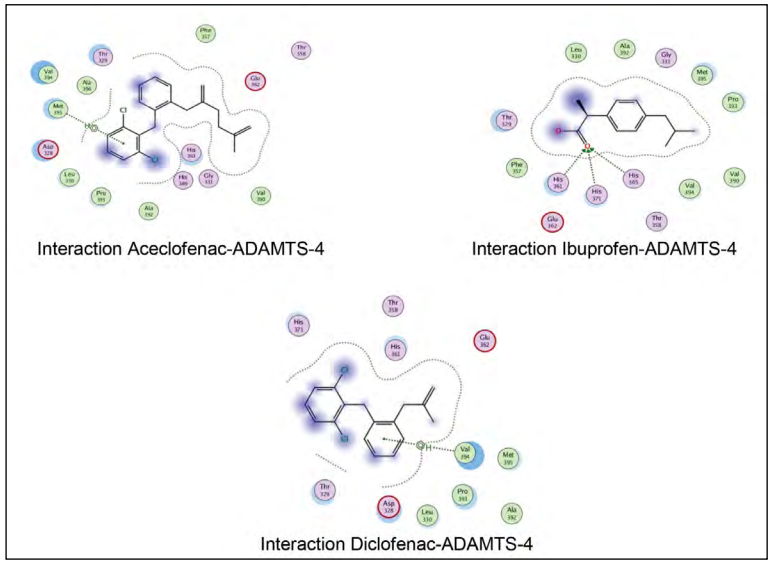

Fig. 9. Interaction between drug ligands and ADAMTS-4

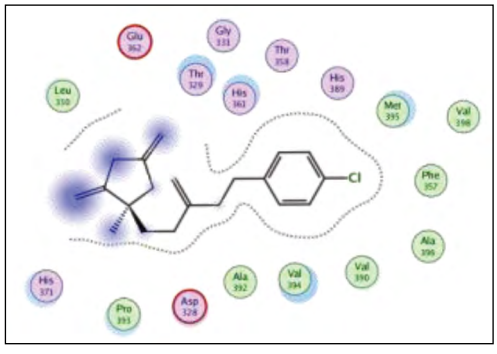

Fig. 10. 2D structure of the complex CHEMBL3358151-ADAMTS-4

For the enzyme aggrecanase-2 (ADAMTS-5), the ligand with the best score 2-Undecanol acetate, Psoralen, and the drug Aceclofenac established a single H-pi interaction with the amino acid HIS410 at the level of the enzyme chain (B), while 2-Nonanol acetate showed no interaction.

Undecan-2-one and Nonan-2-one marked two interactions each; at the chain (B) level with residues LEU379 and HIS410. The Ibuprofen drug had four interactions with HIS410, and Etoricoxib had three interactions, two with the amino acid ILE442 and one is with LEU443. And, finally, the co-crystallisation ligand Marimastat formed two H-donor interactions at the level of the (B) chain of the enzyme with ASP422 and SER441, and an H-acceptor interaction with ARG285 at the chain level (A).

The distances between plant ligands and the active site amino acids of the enzyme ADAMTS-5 range from 2.99 Å to 4.04 Å, while the distances between drugs range from 2.91 Å to 4.75 Å. These results show that the interactions of plant's ligand are slightly better than those of drugs.

The best ligand in score, with an energy of –1.1 kcal/mol and a distance of 3.81 Å implies a fairly weak interaction, unlike Nonan-2-one, which turns out to be a strong interaction with a distance of 2.99 Å and an energy of – 3.4 kcal/mol. The 2D representations of the best pose interactions between the ligands and their receptor ADAMTS-5 are presented in Figs 11–13.

Molecular dynamics simulation

The RMSD is a measure of protein and ligand movement during molecular dynamics. To consider the complex to be stable, it must have an RMSD of less than 2 nm. It is not a rule, but it is a commonly accepted estimate. The

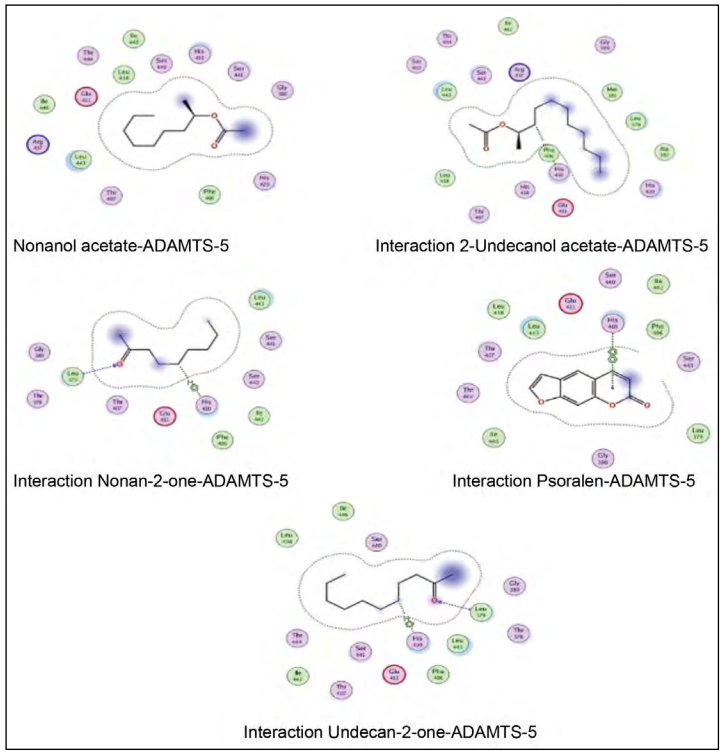

Fig. 11. 2D representations of the best pose interactions between *R. mantana* ligands and ADAMTS-5

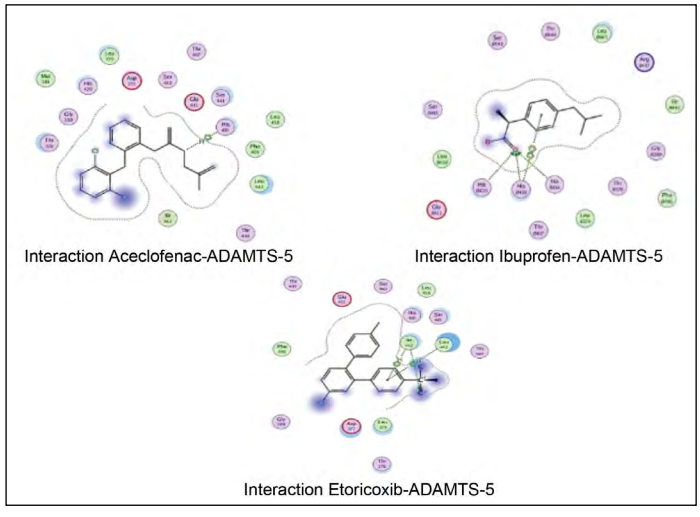

Fig. 12. 2D representations of the best pose interactions between drug ligands and ADAMTS-5

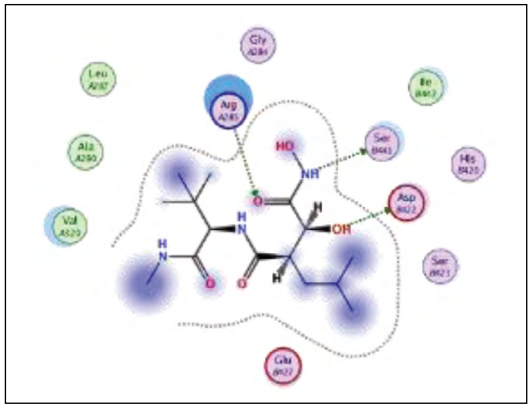

Fig. 13. 2D representations of the best pose interactions between Marimastat and ADAMTS-5

complex with 3HY7 and with an RMSD <1.5 remains stable, while the complex with 4WKE has an increase up to an RMSD 3. The complex with 3HY7 is more stable, although it can also be considered that the other complex is maintained. The results of RMSD of the complex with 3HY7 and 4WKE are presented in Figs 14 and 15.

Evaluation of the amount of hydrogen bonds over time

The complex with 3HY7 forms up to two hydrogen bonds, although at the end of the interaction these are lost; this loss coincides with the increase in RMSD (Fig. 14). In the 4WKE complex, a single hydrogen bridge is maintained until the end of the simulation.

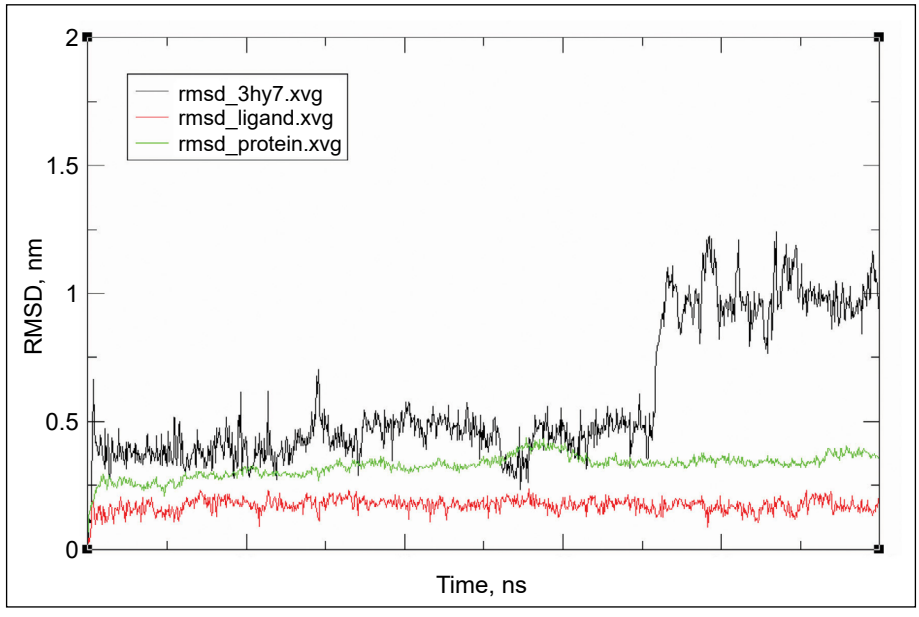

Fig. 14. RMSD of protein, ligand, and complex. 3HY7

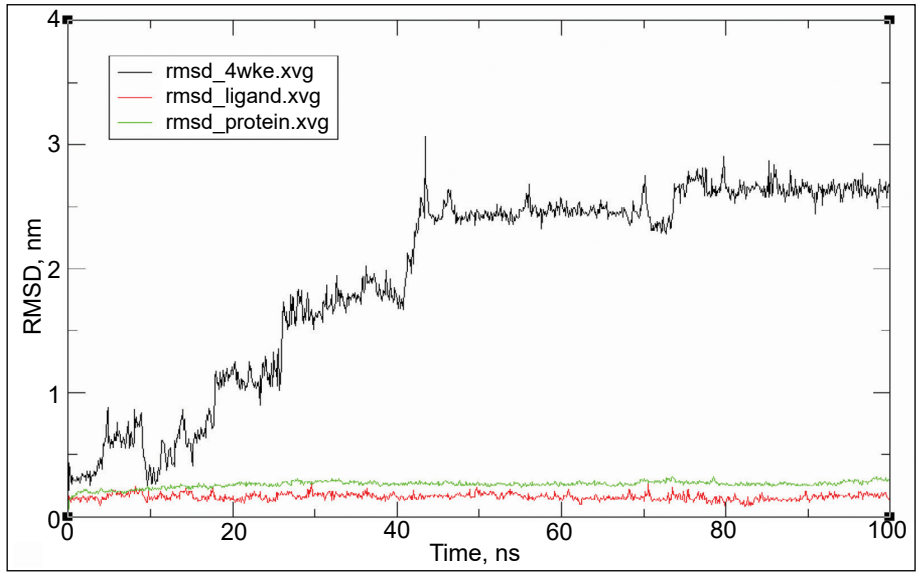

Fig. 15. RMSD of ligand, protein, and complex. 4WKE

Hydrogen bonds of the two complexes are represented in Fig. 16.

Complex RMSF calculation

The RMSF is the degree of fluctuation of the protein considering each atom of the amino acids chain. In the graphs below, the atoms of amino acid chain are on the X axis. These data allow us to detect regions of the protein that have the greatest fluctuation in interaction. In both complexes, regions with high fluctuation can be observed between atoms 1300 and 1500, 2400 and 2600. These regions correspond to those with the greatest movement in the simulation.

Figs 17 and 18 show RMSF of 3HY7 and 4WKE complex.

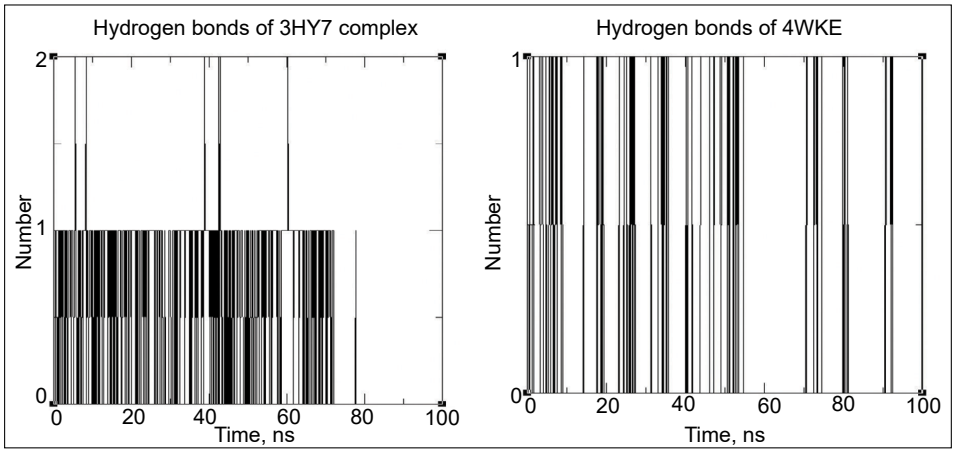

Fig. 16. Hydrogen bonds of 3HY7 and 4WKE complexes

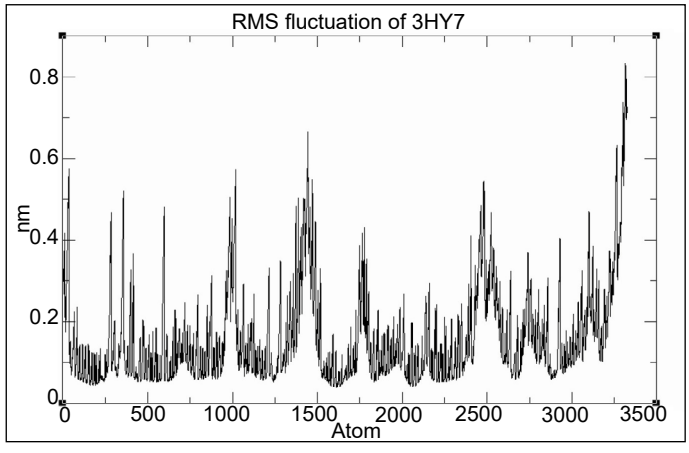

Fig. 17. RMSF of 3HY7

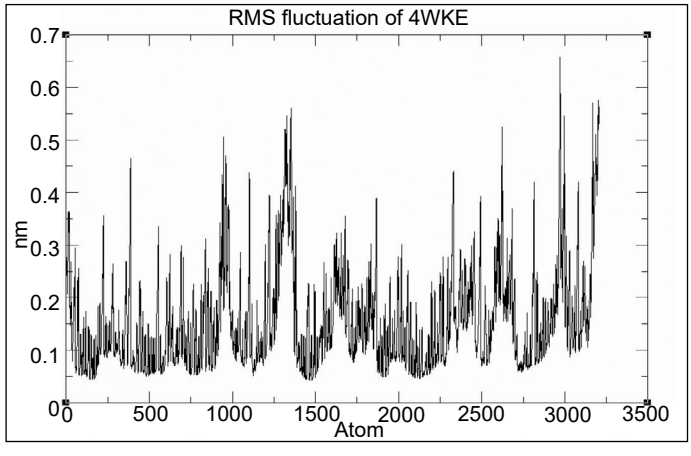

Fig. 18. RMSF of 4WKE

MMPBSA analysis results

The results obtained from the MMPBSA techniques are an evaluation of the total binding free energy, which is the sum of the Van der Waals and electrostatic energies. The binding free energy is calculated in the entire trajectory. There is a higher affinity energy in the complex with 3HY7, but also a higher standard deviation. There is a correlation between the variation of the affinity energy at minute 70 and a movement observed in the RMSD graph (Ihab, 2020). The results are shown in Tables 7 and 8 and Figs 19–20.

Table 7. **MMPBSA of 3HY7 complex**

	Protein-LIG VdW energy [Kcal/mol]	Protein-LIG electrostatic energy [Kcal/mol]	Protein-LIG total energy [Kcal/mol]
Average	–113.3602982	–15.70717679	–129.0674773
Standard deviation	14.26957047	17.75869102	26.05691929
Maximum	–61.32	34.291	–54.031
Minimum	–150.211	–54.551	–187.325

Table 8. **MMPBSA of 4WKE complex**

	Protein-LIG VdW energy [Kcal/mol]	Protein-LIG electrostatic energy [Kcal/mol]	Protein-LIG total energy [Kcal/mol]
Average	–91.54615219	–15.71196387	–107.2581307
Standard deviation	19.18915045	15.22524328	24.70610463
Maximum	–29.09	28.784	–31.107
Minimum	–147.186	–117.661	–182.96

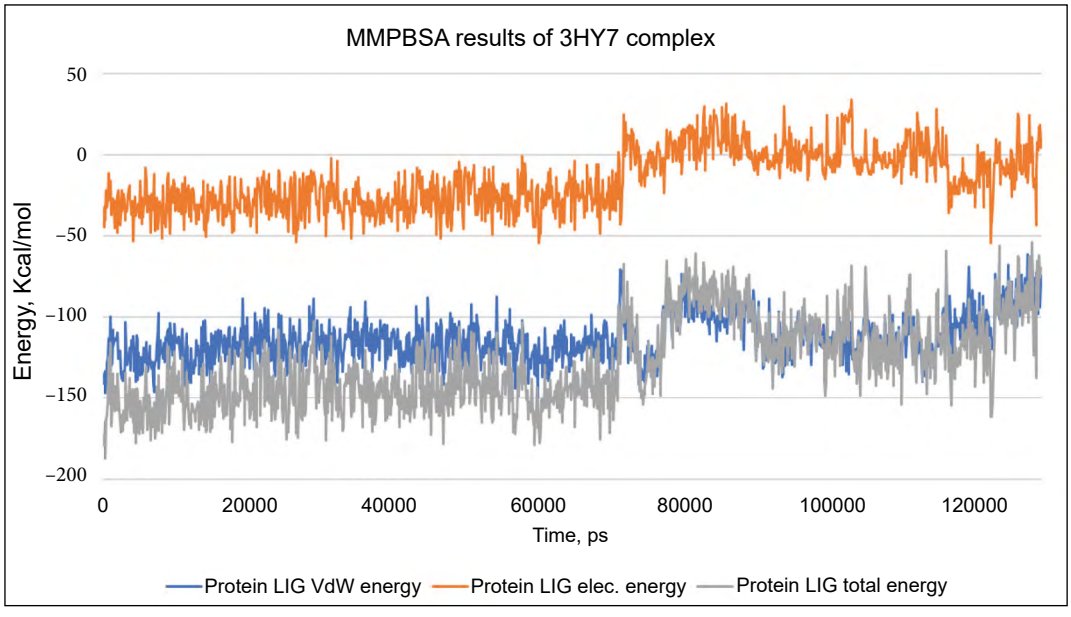

Fig. 19. MMPBSA of 3HY7 complex

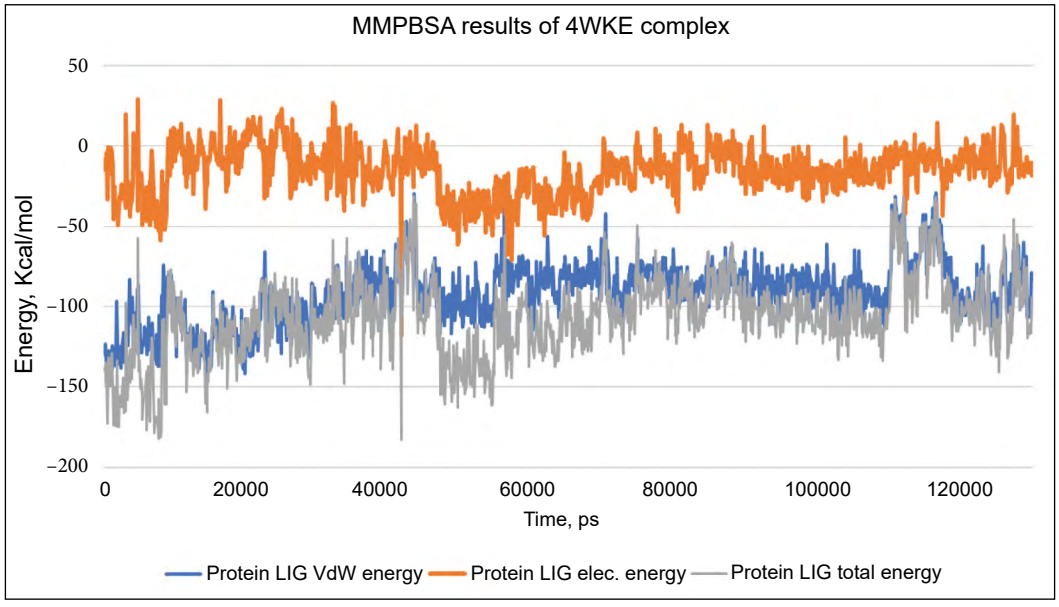

Fig. 20. MMPBSA of 4WKE complex

CONCLUSIONS

The molecular docking method showed the interactions between the plant ligands and aggrecanase. Other experiments on drug-likeness properties, ADME/T tests, PASS prediction, P450 metabolic site (SOM) prediction, and pharmacophore mapping were performed to verify the drug properties of the ligands with the highest yields. The best ligand 2-Undecanol acetate has a high binding affinity (score) for aggrecanase-1 and aggrecanase-2, has three interactions with aggrecanase-1 and one interaction with aggrecanase-2. Our study has shown quite similar and very good results for these natural components with all aspects considered. Therefore, 2-Undecanol acetate can be developed as a candidate drug for osteoarthritis. Finally, we can suggest from this *in silico* study that the component *R. montana* (L.) can inhibit the aggrecanase enzymes and hinder the degradation of articular cartilage. Although these properties are appreciable *in silico*, we encourage the pursuit of other clinical and in vitro studies concerned with osteoarthritis disease.

ACKNOWLEDGEMENTS

We would like to thank everyone who has contributed to this work from near or far.

Received 2 November 2022
Accepted 21 February 2023

References

1. Abraham MJ, Murtola T, Schulz R, Páll S, Smith JC, Hess B, Lindah E. Gromacs: High performance molecular simulations through multi-level parallelism from laptops to supercomputers. SoftwareX. 2015;1–2:19–25. https://doi.org/10.1016/j.softx.2015.06.001
2. Attaf D. Résolution du docking moléculaire: le prototype API-Dock, Algérie, université Mohamed Boudiaf USTO, 2010;16–7.
3. Bussi G, Donadio D, Parrinello M. Canonical sampling through velocity rescaling. J Chem Phys. 2007;126:014101. https://doi.org/10.1063/1.2408420

4. Chen P, Zhu S, Wang Y, Mu Q, Wu Y, Xia Q, Zhang X, Sun H, Tao J, Hu H, Lu P, Ouyang H. The amelioration of cartilage degeneration by ADAMTS-5 inhibitor delivered in a hyaluronic acid hydrogel. Biomaterials. 2014;35:2827–36. doi:10.1016/j.biomaterials.2013.12.076

5. Clément G, Slenzka K. Fundamentals of space biology: research on cells, animals, and plants in space. New York: Springer; 2006.

6. Didierjean C, Tête-Favier F. Introduction to protein science. Architecture, function and genomics. 3rd edition, by Arthu M. Lesk. Oxford University Press: 2016.

7. GROMACS 2021 Source code, 2021. https://doi.org/10.5281/zenodo.4457626

8. HyperChem v8. Molecular Modelling System, Hypercube Inc., 1115 NW 4th Street, Gainesville, FL 32601, USA, 2009.

9. Nour Ihab Sid Ahmed. Histo-morphometric and phytochemical study of *Ruta montana* L. 1756 (Rutaceae) in the region of Tlemcen. 2020.

10. Jo S, Cheng X, Islam SM, Huang L, Rui H, Zhu A, Lee HS, Qi Y, Han W, Vanommeslaeghe K, MacKerell AD, Jr Roux B, Im W. HARMM-GUI PDB manipulator for advanced modeling and simulations of proteins containing nonstandard residues. Adv Protein Chem Struct Biol. 2014;96:235–65. doi:10.1016/bs.apcsb.2014.06.002

11. Jo S, Kim T, Iyer VG, Im W. CHARMM-GUI: a web-based graphical user interface for CHARMM. J Comput Chem. 2008;29:1859–65. doi:10.1002/jcc.20945

12. Juan B, Del Castillo FR, Migel S. Phytochemistry. 1984;23:2095.

13. Kambouche N, Merah B, Bellahouel S, Bouayed J, Dicko A, Derdour A, Younos C, Soulimani C. Chemical composition and antioxidant potential of *Ruta montana* L. essential oil from Algeria. J Comput Chem. 2017;38:1879–86. doi:10.1002/jcc.24829

14. Kim S, Lee J, Jo S, Brooks CL, Lee HS, Im W. CHARMM-GUI ligand reader and modeler for CHARMM force field generation of small molecules. J Comput Chem. 2017;38:1879–86. https://doi.org/10.1002/jcc.24829

15. Kumari R, Kumar R, Open Source Drug Discovery Consortium, Lynn A. g-mmpbsa – a GROMACS tool for high-throughput MM-PBSA calculations. J Chem Inf Model. 2014;54:1951–62. https://doi.org/10.1021/ci500020m

16. Kuzovkina IN, Szarka SZ, Héthelyi E, Lemberkovics E, Szöke E. Composition of essential oil in genetically transformed roots of *Ruta graveolens*. Russ J Plant Physiol. 2009;56:846–51. https://doi.org/10.1134/S1021443709060156

17. Lee J, Cheng X, Swails JM, Yeom MS, Eastman PK, Lemkul JA, Wei S, Buckner J, Jeong JC, Qi Y, Jo S, Pande VS, Case DA, Brooks CL, MacKerell AD, Klauda JB, Im W. CHARMM-GUI Input Generator for NAMD, GROMACS, AMBER, OpenMM, and CHARMM/OpenMM Simulations Using the CHARMM36 Additive Force Field. Chem Theory Comput. 2016;12(1):405–13. doi:10.1021/acs.jctc.5b00935

18. Malfait AM, Arner EC, Song RH, Alston JT, Markosyan S, Staten N, Yang Z, Griggs DW, Tortorella MD. Proprotein convertase activation of aggrecanases in cartilage in situ. Arch Biochem Biophys. 2008;478(1):43–51. doi:10.1016/j.abb.2008.07.012

19. Mejri J, Manef A, Mejri M. Chemical composition of the essential oil of *Ruta chalepensis* L.: Influence of drying hydrodistillation duration and plant parts. Ind Crops Prod. 2010;32:671–3. https://doi.org/10.1016/j.indcrop.2010.05.002

20. Mohhr N, Budzi KH, Tawil BAH. 1982. Phytochemistry, 7(9).

21. Neogi T. The epidemiology and impact of pain in osteoarthritis. Osteoarthritis Cartilage. 2013;21:1145–53. doi:10.1016/j.joca.2013.03.018

22. O'Boyle NM, Banck M, James CA, Morley C, Vandermeersch T, Hutchison GR. Open Babel: An open chemical toolbox. J Cheminform. 2011;3:33. doi:10.1186/1758-2946-3-33

23. Raghav SK, Gupta B, Agrawal C, Goswami K, Das HR. Anti-inflammatory effect of *Ruta graveolens* L. in murine macrophage cells. J Ethnopharmacol. 2006;104:234–9. doi:10.1016/j.jep.2005.09.008

24. Tanuja J, Tushar J, Hemlata P, Priyanka S, Shalini M, Subhash C. Predictive modeling by deep learning, virtual screening and molecular dynamics study of natural compounds against SRAS-CoV-2 main protease. J Biomol Struct Dyn. 2021;39:6728–46. doi:10.1080/07391102.2020.1802341

25. Trouillas P. Les interactions ligand-récepteur et la modélisation moléculaire, Limoges, France, 2011.

26. Vanommeslaeghe K, Hatcher E, Acharya C, Kundu S, Zhong S, Shim J, Darian E, Guvench O, Lopes P, Vorobyov I, Mackerell AD Jr, CHARMM general force field: a force field for drug-like molecules compatible with the CHARMM all-atom additive biological force fields. J Comput Chem. 2010;31:671–90. doi:10.1002/jcc.21367

27. Vincent TL, McClurg O, Troeberg L. The extracellular matrix of articular cartilage controls the bioavailability of pericellular matrix-bound growth factors to drive tissue homeostasis and repair. Int J Mol Sci. 2022;23:6003. doi:10.3390/ijms23116003

Imane Abdelli, Faiçal Hassani, Sarra Ghalem, Sohayb Bekkal Brikci, Ihab Sid Ahmed Nour, Andrés Reyes Chaparro, Amina Belhadji, Mohamed El Hadi Ghalem, Karim Ferouani

RUTA MONTANA L. FITOCHEMINIŲ KOMPONENTŲ SLOPINAMOJO AKTYVUMO PATIKRA SIEKIANT SUMAŽINTI OSTEOARTRITO LIGOS VYSTYMĄSI: *IN SILICO* TYRIMAS

Santrauka

Ruta montana L. rūšis yra gerai žinoma dėl savo gydomųjų savybių. Rūtos augalas naudojamas tradicinėje medicinoje, daugybė jo fiziologiškai aktyvių cheminių medžiagų turi gydomąjį potencialą. Atlikti *in silico* tyrimai su *R. montana* ligandų molekulėmis rodo, kad šie junginiai slopina fermentus, atsakingus už osteoartrito ligos agrekanazės-1 (ADAMTS-4) ir agrekanazės-2 (ADAMTS-5) degradaciją žmogaus sąnarių kremzlėje. Taikant molekulinio prijungimo modeliavimą, buvo nustatyta *R. montana* augalo ligandų molekulių ir šių fermentų sąveika. Atliekant 2-undekanolio acetato, 2-nonanolio acetato, nonan-2-ono, psoraleno ir undekano-2-ono komponentų *in silico* tyrimus, šie junginiai įvertinti aukštesniais balais, ir tai patvirtina didesnį jų slopinamąjį aktyvumą, palyginti su galimais komerciniais vaistais nuo osteoartrito.

Raktažodžiai: *Ruta montana* L. komponentai, osteoartritas, agrekanazė-1 (ADAMTS-4), arekanazė-2 (ADAMTS-5), molekulinio prijungimo modeliavimas